Available online at www.sciencedirect.com

ScienceDirect

Procedia Manufacturing 00 (2019) 000–000

Procedia MANUFACTURING

www.elsevier.com/locate/procedia

18th International Conference Metal Forming 2020 Project

2D thermal finite element analysis of sticker breakout in continuous casting.

Hoang-Son Tran[a], Etienne Castiaux[b], Anne-Marie Habraken[a,c,*]

[a]*University of Liege (ULiege), ArGEnCo Dpt, Materials and Solid Mechanics Unit, Allée de la Découverte, 9 B52/3, B 4000 Liège, Belgium*
[b]*EBDS Engineering S.p.r.l. 39 Avenue du Progrès,B-4100 Seraing*
[c]*F.R.S.-FNRS, Fonds de la Recherche Scientifique, Rue d'Egmont 5, B 1000 Bruxelles, Belgium*

* Corresponding author. Tel.: +32 4 3669430; *E-mail address:* Anne.Habraken@uliege.be

Abstract

The sticker breakout is an accident in continuous casting which could frequently occur without a correct process monitoring. The breakout of the sticker has become one of the main factors limiting the development of the continuous casting technology at high speed and wide-thick-plate. In this work, finite element models of the steel shell formation in continuous casting have been developed. The thermal parameters such as conductivity of mold, convection due to cooling system, thermal contact resistance were calibrated. The model allows to predict the temperature field throughout the process. The prediction of shell thickness reasonably agrees with experimental observations. Then, a 2D-thermal model of sticker breakout is established. The new algorithm allows for prediction of hot tearing due to sticking phenomena and its propagation. Current simulations are useful to define the model sensitivity and they increase the understanding of this phenomena.

Keywords: Continuous casting; Sticking breakout; Thermal analysis; Lagamine; Finite element.

1. Introduction

In recent times, the production of metals by the continuous casting process keeps growing; the main reasons are the product quality and the cost-effectiveness. Within this process, liquid steel is poured into a mold which is kept at a medium temperature thanks to a cooling system. The molten metals in contact with the mold quickly start to solidify. Extracting rolls pull the strand and keep it moving forward in the caster while water continues cooling it. The strand can be cut when the section is solidified. Once a fracture happens due to the sticking of the solid shell near meniscus, the propagation of crack begins is a cyclic event staggered in space and in time. It consists of 2 main steps: a crack due to sticking of solid shell is formed. The gap is filled by liquid steel which is solidified and increases the area already stuck on the mold. The thin, hot and weak layer just formed at the crack location will be teared again in shifted a location toward the casting direction due to the relative movements of the mould and the strand Fig.1. This phenomenon not only affects the smooth production of continuous casting but also damages equipment.

Many parameters affect the process such as: composition of the steel, mold level, superheat temperature, cooling conditions, mold oscillation, casting speed... Therefore, numerical methods are useful to increases the understanding of continuous casting process.

Some analytical solutions for the development of the stress field in the strand in the course of solidification were developed by Weiner and Boley [1], as well as by Tien and Kaump [2]. Even though these analytical solutions provide reference results for the verification of other numerical models, they are often unable to provide accurate information in real industrial applications presenting defects. Those model assumptions are too simple for the various complex physical phenomena associated with the process. Therefore, to provide more accurate models and generate new numerical analyses become crucial. Hattel and his collaborators [3] proposed the finite volume difference method to simulate three-dimensional

thermo-elastic stresses. Jung-Eui Lee et al. [4] used a finite volume method for the coupled fluids flow problem. Heinlen et al. [5] used the boundary element method to predict the behaviour in one-dimensional solidification of aluminum.

The finite element method (FE) is an approach particularly adapted to the problem of a wide variety of non-linearities and geometric shapes. For that reason, many researchers use this method to study this continuous casting process. In 2D cases, it has been applied to simulate shell thinning breakouts [6], ideal taper optimization [7], and stresses during solidification process [8-12]. Koric et al. developed a full 3D thermo-mechanical model of solidified shell [13]. Recently, Zhang et al. developed a coupled simulation of fluid flow and stress-strain analysis for continuous casting [14]. However to the authors' knowledge, no FE simulation simulates the sticking breakout problem.

In this study, we report an application of a 2D thermal finite element model to predict temperature field throughout the process. Then, the first model of sticker breakout phenomena is presented. This work is based on the Lagamine code of the MSM group of the University of Liege which has been previously applied on the modeling of the continuous casting process [15-16].

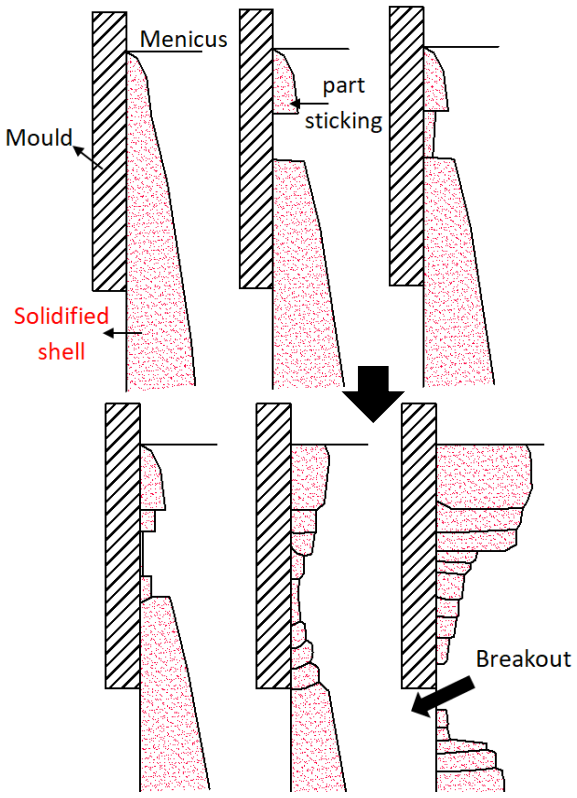

Fig.1. The propagation of a crack due to the sticking breakout phenomenon.

2. Model Description

2.1. Heat transfer finite element analysis

Two types of laws are required in the thermal modeling approach: (i) bulk heat transfer by conduction, including the heat accumulation in the solid and (ii) surface heat transfer by convection and radiation. The classical non-linear equation of conduction is:

$$\frac{\partial}{\partial x}\left(k\frac{\partial T}{\partial x}\right)+\frac{\partial}{\partial y}\left(k\frac{\partial T}{\partial y}\right)+Q_{\text{int}}=\rho c_p\frac{\partial T}{\partial t} \quad (1)$$

with the temperature $T(x,y,t)$ $[K]$, the thermal conductivity $k(T)$ $[W.m^{-1}.K^{-1}]$, $c_p(T)$ $[J.Kg^{-1}.K^{-1}]$ the apparent heat capacity, $\rho(T)$ $[kg.m^{-3}]$ the density, Q_{int} $[W.m^{-3}]$ the power generated per volume in the work-piece, and finally t the time. Heat exchange by convection and radiation is defined by:

$$-k(\nabla T.n)=-h(T-T_0)-\varepsilon\sigma(T^4-T_0^4) \quad (2)$$

where h is the convection coefficient [$W.m^{-2}.K^{-1}$], σ is the Stefan-Boltzman constant ($5.67\times10^{-8}W.m^{-2}.K^{-4}$), ε is the emissivity coefficient, T_0 is the initial temperature

The latent heat of solidification is integrated in the definition of c_p. All the data related to the thermo-physical properties of the slab are recovered from [15]

The heat exchange depends on the contact conditions between the strand and the mold. In thermo-mechanical analysis, contact can be lost in some places due to the thermal shrinkage and the thermal exchange will be decreased. However, in the current thermal model, the contact between the mold and the strand is assumed always established, the heat transfer is given by

$$q_{\text{contact}} = R\ .\ (T_{\text{strand}} - T_{\text{mold}}) \quad (3)$$

with R the contact thermal resistance (mW/mm^2K), T_{strand} and T_{mold} the absolute temperatures (K) of the strand and the mold respectively

2.2. Finite element model

In order to simulate the crack propagation due to the sticking phenomenon, our simulation procedure consists of two stages: a first thermal model to reach the stationary state and then a second model to take into account the sticking phenomenon and the crack propagation. The 2D vertical section studied corresponds to a middle section of the system. By symmetry, the mesh of the slab concerns its half thickness (see Fig.2). The meshed mould consists of a 40mm thick copper bloc cooled by its outer face. In reality, the mould is cooled by a circulation of water, here the radiation convection exchanges are adjusted to reproduce a realistic thermal field within the mould.

Fig.3 shows the dimension of the finite element mesh for the first stage. The copper mold and the steel are modeled using quadrilateral elements with 4 nodes and 1 integration point. The elements are refined in the area near the contact between the mold and the steel. This mesh contains 18969 solid elements and 18846 nodes, the size of the slab refined

elements is 2mmx2mm and that of the mold is 3mmx3mm. The contact between the mold and the slab is simulated by contact elements [17]. The thermal capacity of the copper is 2776 mJ / mm³ and assumed to be constant with temperature. The radiation coefficient is 10^{-8} W.m^{-2}.K^{-4} on the external face of the mold. Two sets of thermal conductivity parameters of the mold (Fig.4): Set 1 [18] and Set 2 [19] will be verified. The convection coefficient and thermal contact resistance are adjusted to recover the temperature experimentally observed within the mold by our industrial partner.

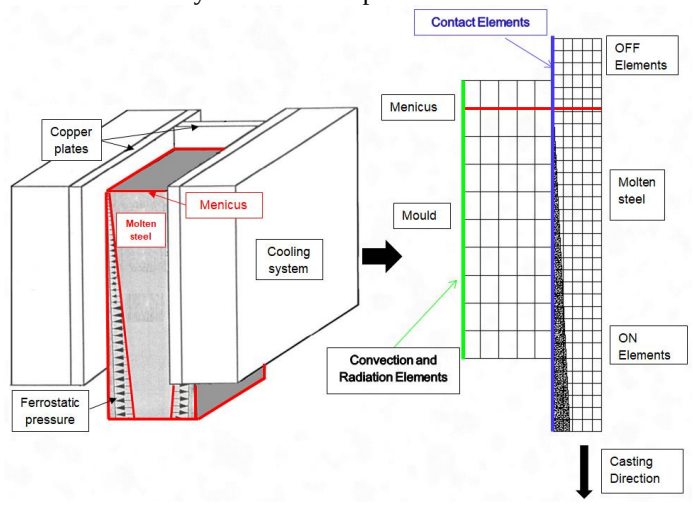

Fig.2. Illustration of the 2D finite element strategy of continuous casting.

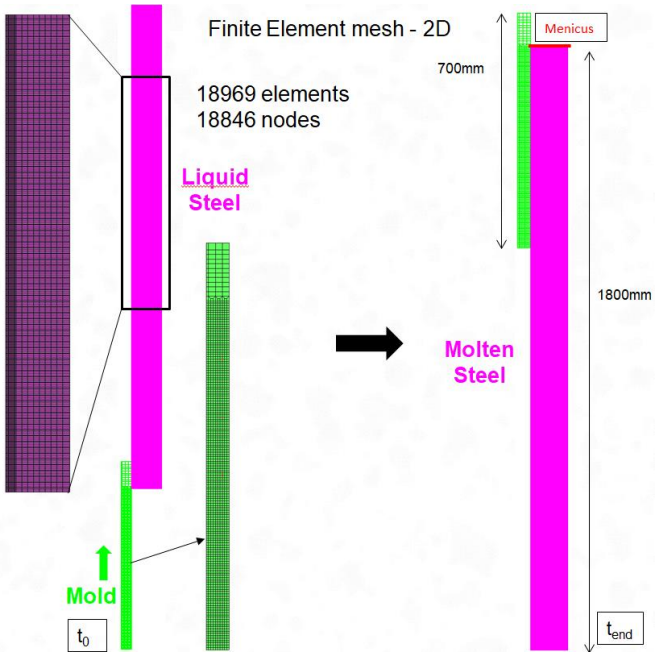

Fig.3. Mesh used to calculate the thickness of the solidified strand.

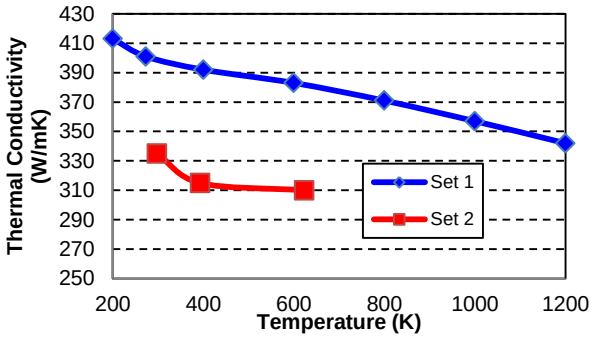

Fig.4. Two sets of thermal conductivity of mold.

3. Calibration of the thermal model

3.1. Result of reference parameters

Fig.5b and Fig.5c shows the distribution of the calculated temperature of the mold wall and the strand (dark red is liquid, dark blue is solid) with the first set of thermal conductivity of copper, h=4 mW/mm²K, and $R_{contact}$ = 5 mW/mm²K and $V_{casting}$ =1.3m/min. One observes an increase of the solidified layer thickness under the meniscus. The predicted temperature values within the mold for 3 positions of thermocouples have been compared with reference experimental values and are shown in Fig.6. The predicted temperatures are much higher than the reference values at steady casting state. These differences (>150°C) could have been caused by numerous factors. For that reason, in the next sections, we present the sensitivity analysis of input parameters such as: the choice of the convection coefficient of the mold replacing true cooling effect of water circulation; the thermal contact resistance between the mold and the strand; the thermal conductivity of the mold.

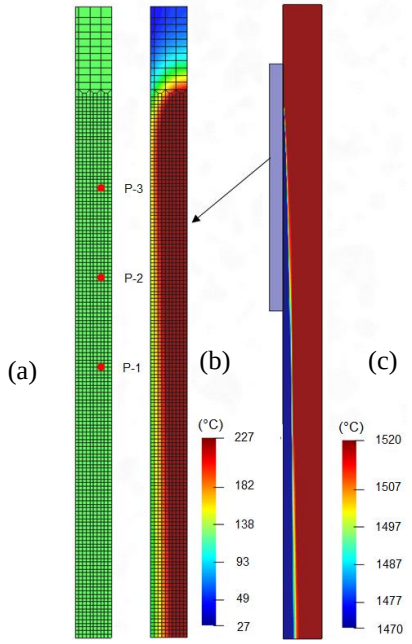

Fig.5. (a) Position of thermo couple; (b) temperature distribution of mold at 60s; (c) temperature distribution of strand at 60s.

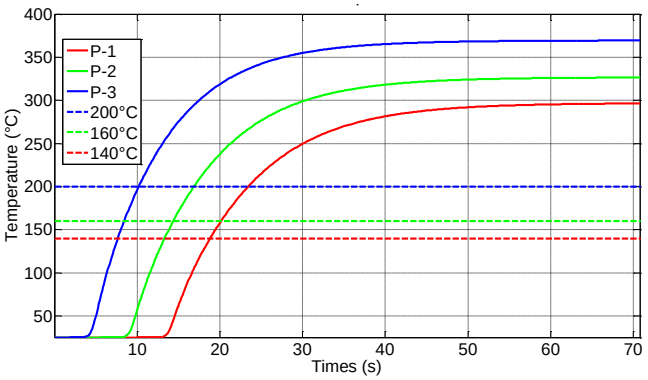

Fig.6. Temperature at 3 measuring points of thermocouple and its corresponding reference values (same color).

3.2. Influence of the conductivity parameters of mold

In this section, the effect of the chosen thermal conductivity parameter of the mold on the predicted temperature within the mold wall is presented. Numerical simulations were run with the 2 different conductivity parameters from Fig.4. One finds that the thermal history at the thermocouple of set 2 reaches a plateau earlier than set 1. The predicted temperatures are also higher (see Fig.7). The obtained results show a high sensitivity to the conductivity parameter. Hereafter, this first set of parameters will be used to predict the thermal field during the whole continuous casting process.

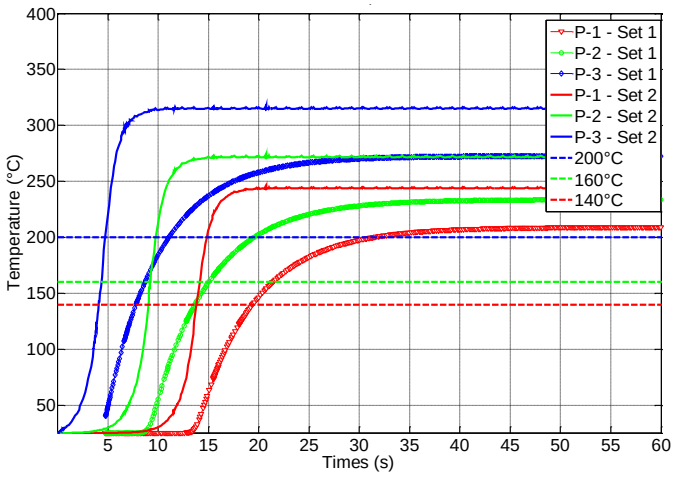

Fig.7. Sensitivity of temperature history due to thermal conductivity parameter at the location of 3 thermocouples.

3.3. Influence of Convection parameters

Fig.8 shows of course a strong sensitivity of the temperature within the mold wall to the boundary condition defined by the convection coefficient. The calculated temperature decrease with increasing coefficient of convection. However, these results indicate that this effect reach a saturation level for the coefficient value h=5000 mW/mm²K. Therefore, this parameter will be used for further simulations.

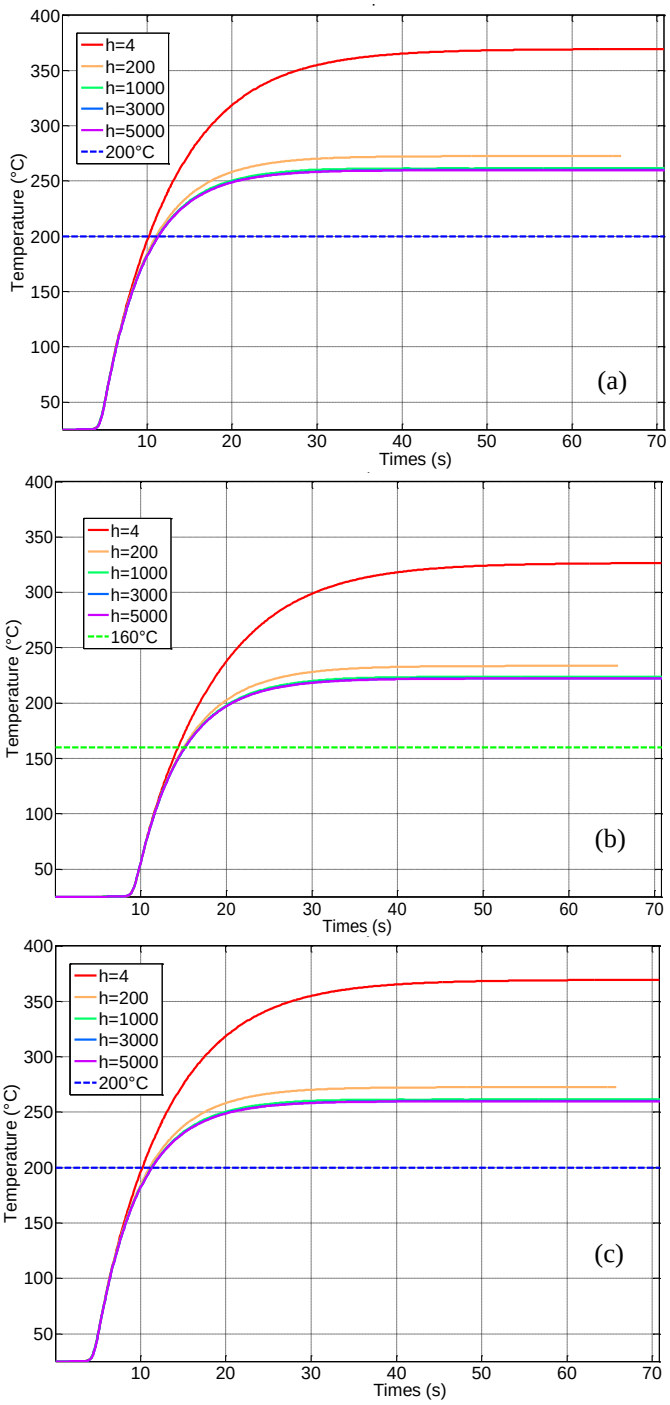

Fig.8. (a) Sensitivity of temperature history due to convection coefficient on outer face of the mold at Point 1; (b) Point 2; (c) Point 3.

3.4. Influence of the contact thermal resistance

In this section, the effect of thermal contact resistance $R_{contact}$ is presented. Several simulations were run with different resistance parameters. One finds that calculated temperature values increase with increasing $R_{contact}$ coefficient of these parameters (see Fig.9). The results obtained with $R_{contact}$ = 2,65 mW/mm²K match the third thermocouple

reference value and the errors at 1st and 2nd thermocouple are less than 30°C. The sensitivity study shows that to accurately capture the thermal behavior of Continous Casting process by FE model, both the convection coefficient and the thermal contact resistance must be correctly calibrated. Hereafter, the set of parameters: $R_{contact}$ = 2,65 mW/mm²K and h=5000mW/mm² will be used for our further studies.

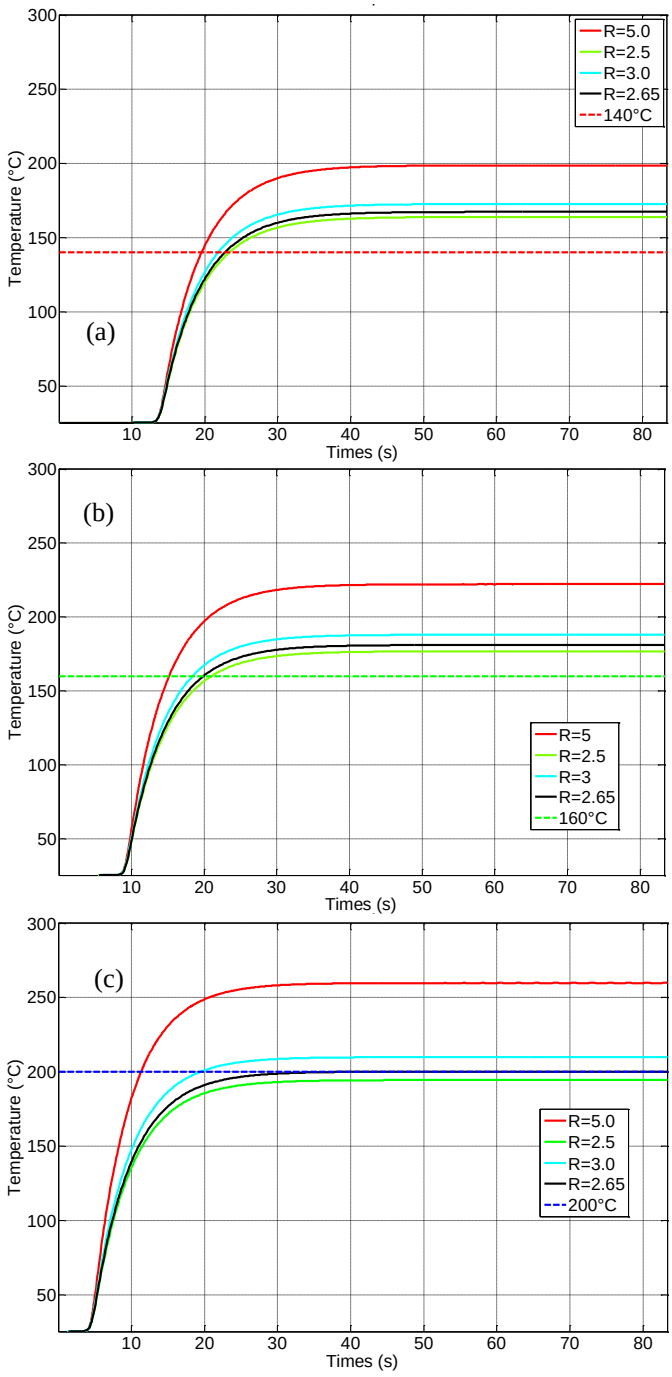

Fig.9. (a) Sensitivity of temperature history due to thermal contact resistance coefficient between the mold and the strand at Point 1; (b) Point 2 (c) Point 3.

4. Result of stationary state simulations

4.1. Temperature predicted with calibrated parameters

The continuous casting process data are as follows: temperature of the incoming steel in the mould TL=1793K; casting speed $V_{casting}$ =1.3m/min; $R_{contact}$ = 2,65 mW/mm²K; h=5000mW/mm². Fig.10 shows the temperature distribution in the mold wall and the strand at the stationary state of process. The temperature of the mold rapidly decreases from liquid steel contact face to outer face. The temperature near the meniscus is of course higher than within the bottom part due to the cooling mold effect. The shell thicknesses of the solidified steel d_{shell}=17mm at the exit of mold is in agreement with industrial observations. Fig.11 indicates the predicted temperature on positions of thermocouples is in reasonable agreement with the measured values; the greatest temperature difference is 30°C which is not significant due to the variation of the experimental results.

The industrial conditions do not allow accurate position of thermocouples and the simulation goal is just to be representative of a general cooling case (to model accurate geometry of mold is not the target)

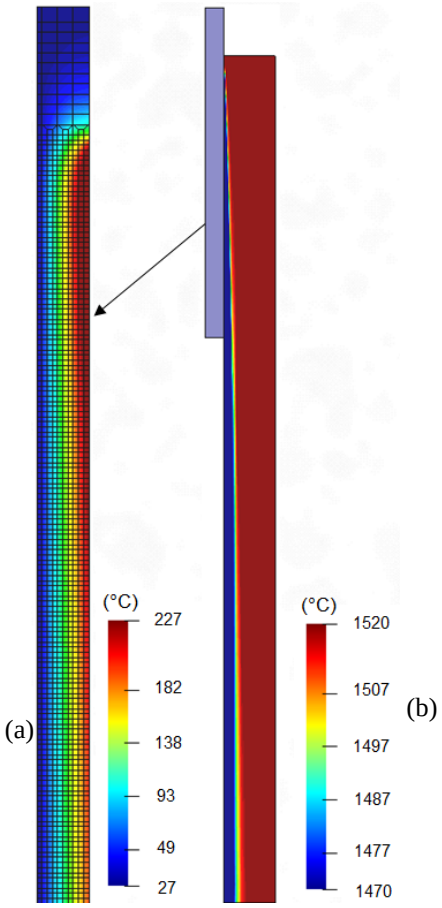

Fig.10. (a) Temperature field of the mold at 83s; (b) Temperature field of the strand at 83s.

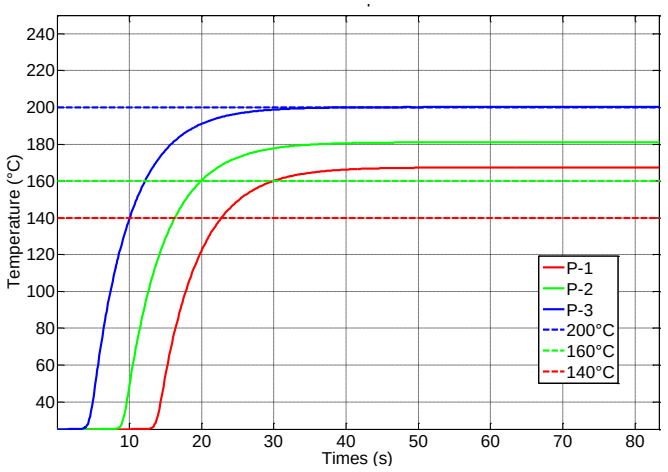

Fig.11 Computed temperature values at 3 thermocouple and their corresponding experimental values (same color).

4.2. Effect of Casting Speed on solidified layer thickness

In industrial practice, the understanding of the effect of casting speed on the mold and strand temperature is the required to monitor the process by automatic ways and to teach the operators. Fig.12 shows the effect of the casting speed on the solidified layer thickness of the strand at the mold exit. The thickness decrease with increasing casting speed is obvious. The shell thicknesses of the solidified steel in the range of 14mm to 25mm which is in good agreement with the industrial data.

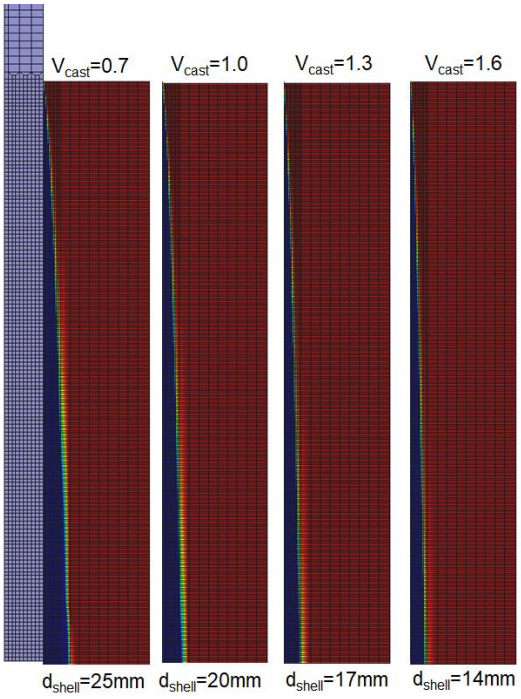

Fig.12. Effect of the casting speed (m/min) on the thickness of the solidified shell (dark red liquid, dark blue solid).

5. Results of sticker break out simulation

5.1. Sticker breakout simulation

In the first model stage, the thermal simulation is performed to reach the stationary state. Then a manual projection is applied from the original model to a new thermal model Fig.13. This new mesh is designed to give sufficient refinement in the future fracture area. Then the sticking model begins.

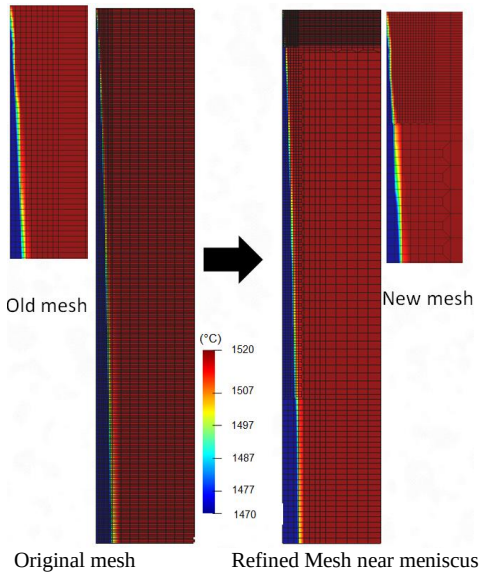

Fig.13. The thermal fields in the old mesh and in the new mesh (dark red liquid, dark blue solid).

A remeshing procedure has been developed to specifically take into account the sticking phenomena and its propagation. At the current of stage study, the mechanical effect is not yet modeled. One can assume that the amplitude of the tear is constraint by the difference in relative displacement of the mold and the strand. The 2D remeshing procedure is applied after each period of oscillation T [20]. When the mold goes up, the sticking part of the strand accompanies the mold, and then the strand will be teared at the weakest point below the sticking part. In our procedure, the first sticking part is imposed by a rigid body displacement d for each period by:

$$d=V_{casting}\times T \quad (4)$$

The new layers of liquid steel elements are introduced below the section of crack. These elements are in direct contact with the mold and so quickly solidify. The solidification time duration will be studied in future studies. In fact, the new solidified shell is mechanically the weakest, and a new crack will be detected by a thermal criterion where the solidified shell thickness is the smallest. Finally, the sticking part goes up and re-tears the strand again below the old crack. The phenomenon is repeated and enables the crack to propagate (see Fig.14). For each new mesh, several information needs to be updated such as: temperature of new nodes, contact elements, boundary conditions.

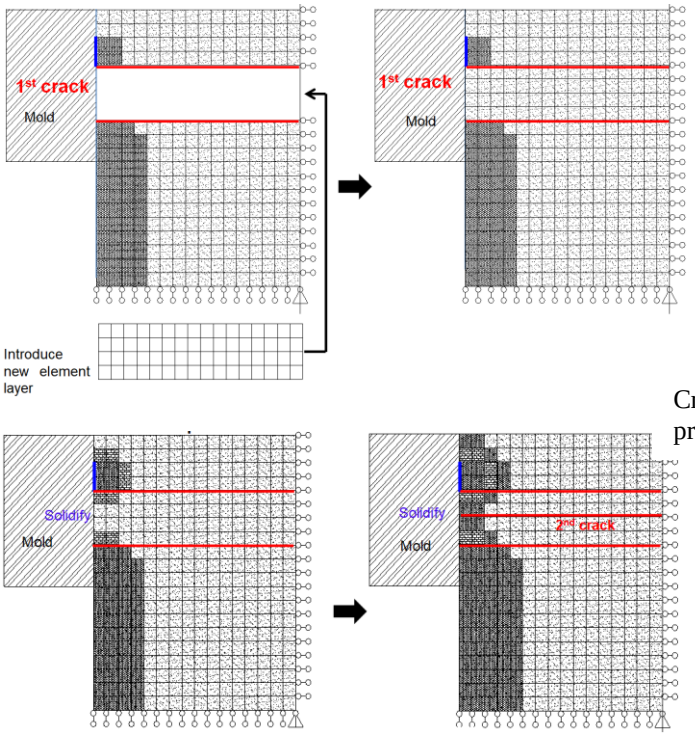

Fig.14. Description of the methodology to add elements at the crack event and to follow the crack propagation.

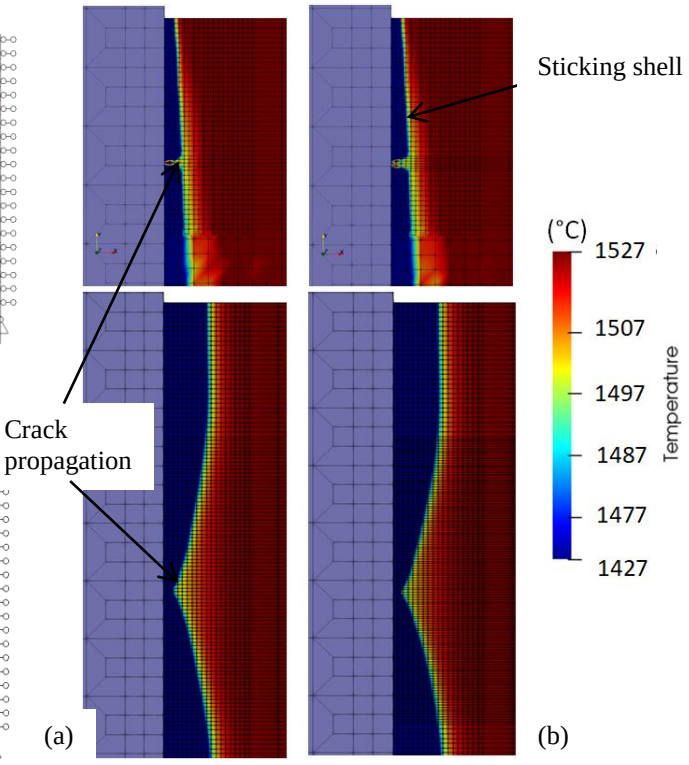

Fig.15. Finite element model of sticking break out phenomenon (a) coarse add mesh (b) fine add mesh.

5.2. Influence of the refinement of the added elements

Currently, the sticking thermal model robustness and sensitivity are tested in order to validate the method. The continuous casting process data are as follows: the casting speed $V_{casting}$ =1mm/s; oscillation period T=1s; "Negative time strip" = 0,25s [20]. Fig.15 shows the propagation of crack due to a sticking shell with 2 different sizes of new elements. We observe a very small difference between the two predicted thermal fields (same solid thickness at similar time). This model could help to understand and optimize repair procedure of sticking breakout problem.

6. Conclusion

In the present paper, a 2D thermal finite element approach models the stationary state of a continuous casting process. It allows predicting the thermal field within the mold wall and the thickness of the solidified steel shell of the strand. A second thermal model is established in order to simulate the propagation of a crack due to the sticking break out phenomenon. A specific remeshing procedure has been developed. The model allows predicting hot tearing due to sticking phenomena and its propagation. The model sensitivity has been checked. It increases the understanding of the phenomena. In future work, parametric studies of crack events will improve the knowledge of this phenomenon and a 3D mechanical approach will help to identify the mechanical stress and strain fields in 3D at the rupture events.

Acknowledgements

As Research Director of FRS-FNRS, AM Habraken acknowledges the support of this institution. The Walloon Region, specifically the Pole Mechatech program and EBDS Engineering S.p.r.l. are thanked for their financial support of the project: ECA - Convention n° 7901.

References

[1] Weiner JH, Boley BA. Elasto-plastic thermal stresses in a solidifying body. Journal of the Mechanics and Physics of Solids 1963;11(3):145-54.
[2] Tien RH, Koump V. Thermal Stresses During Solidification on Basis of Elastic Model. Journal of Applied Mechanics 1969 Dec 1;36(4):763-7.
[3] Hattel J, Hansen PN, Hansen LF. Analysis of thermal induced stresses in die casting using a novel control volume FDM technique. 1993;585-92.
[4] Lee JE, Yeo TJ, Hwan OH K, Yoon JK, Yoon US. Prediction of cracks in continuously cast steel beam blank through fully coupled analysis of fluid flow, heat transfer, and deformation behavior of a solidifying shell. Metallurgical and Materials Transactions A 2000;31(1):225-37.
[5] Heinlein M, Mukherjee S, Richmond O. A boundary element method analysis of temperature fields and stresses during solidification. Acta Mechanica 1986;59(1):59-81.
[6] Moitra A. Thermo-mechanical model of steel shell behavior in continuous slab casting University of Illinois at Urbana-Champaign; 1993.
[7] Thomas B, Moitra A, Mcdavid R. Simulation of longitudinal Off-corner depressions in continuously cast steel slabs. 23 ed; 1996.
[8] Park JK, Thomas BG, Samarasekera IV. Analysis of thermomechanical behaviour in billet casting with different mould corner radii. Ironmaking & Steelmaking 2002 Oct 1;29(5):359-75.

[9] Park J-K, Li C, Thomas BG, Samarasekera IV. Analysis of Thermo-Mechanical Behavior in Billet Casting. 60th Electric Furnace Conference, San Antonio, TX, Nov. 10-12, ISS-AIME, Warrendale, PA, 669-685, 2002.

[10] Tszeng TC, Kobayashi S. Stress analysis in solidification processes: Application to continuous casting. International Journal of Machine Tools and Manufacture 1989;29(1):121-40.

[11] Boehmer JR, Funk G, Jordan M, Fett FN. Strategies for coupled analysis of thermal strain history during continuous solidification processes. Advances in Engineering Software 1998;29(7):679-97.

[12] Boehmer JR, Fett FN, Funk G. Analysis of high-temperature behaviour of solidified material within a continuous casting machine. 1993;47(4-5):683-98.

[13] Koric S, Thomas BG. Efficient thermo-mechanical model for solidification processes. Int J Numer Meth Engng 2006 Jun 18;66(12):1955-89.

[14] Zhang S, Guillemot G, Gandin CA, Bellet M. A partitioned solution algorithm for fluid flow and stress-strain computations applied to continuous casting. 2019;529:012082.

[15] Pascon F, Habraken AM . Finite element study of the effect of some local defects on the risk of transverse cracking in continuous casting of steel slabs. Computer Methods in Applied Mechanics & Engineering, 2007; 196, 2285-5599.

[16] Pascon F, Pecquet E, Zhang L, Habraken AM. Modelling of semi-continuous casting of cupro-nickel alloys. Papadrakakis, M., Onate, E., and Schrefler, B. Proceedings of the International Conference on Computational Methods for Coupled Problems in Science and Engineering; 2005.

[17] Habraken AM, Cescotto S. Contact between deformable solids, the fully coupled approach. Mathematical and Computer Modelling. 1998; 28(4-8), 153-169.

[18] https://www.engineeringtoolbox.com/thermal-conductivity-metals-d_858.html.

[19] Meng X, Zhu M. Thermal Behavior of Hot Copper Plates for Slab Continuous Casting Mold with High Casting Speed. ISIJ International. 2009; 49(9):1356-61.

[20] Tran H. S., Castiaux E., Habraken A. M. Thermal analysis of solidifying steel shell in continuous casting process. 23rd International Conference on Material Forming (ESAFORM 2020), Cottbus (Germany), 4 – 6 May 2020.